



# Design and Characterization of Piezoceramic Thick Film Sensor for Measuring Cutting Forces in Turning Processes

M. Panesso<sup>1</sup>(✉), M. Ettrichrätz<sup>1</sup>, S. Gebhardt<sup>2</sup>, O. Georgi<sup>1</sup>, C. Rüger<sup>1</sup>, M. Gnauck<sup>1</sup>, and W.-G. Drossel<sup>1</sup>

<sup>1</sup> Fraunhofer IWU, Fraunhofer Institute for Machine Tools and Forming Technology, Nöthnitzer Str. 44, 01187 Dresden, Germany

miguel.antonio.panesso.perez@iwu.fraunhofer.de

<sup>2</sup> Fraunhofer IKTS, Fraunhofer Institute for Ceramic Technologies and Systems, Winterbergstr. 28, 01277 Dresden, Germany

**Abstract.** Cutting forces in turning processes usually correlate with tool conditions. For this reason, the acquisition of force signals is of key importance for monitoring purposes. Despite the robustness of current piezoelectric measuring platforms, their large weight ratio relative to standalone tool-holder systems limits their effective usable bandwidth for analyzing force signals. Further limitations include high costs and lack of flexibility for general purpose turning operations. Due to this, such systems fail to find acceptance in practical applications and are mainly limited to research activities. To improve these aspects, this work investigates the use of an alternative integration concept using a piezoceramic thick film sensor for performing near-process cutting force measurements at the tool-holder. The charge output of the sensor was estimated using a coupled structural-piezoelectric simulation for its design. The modelled prototype was assembled and characterized by means of a static calibration and an impact hammer test. Following these, a first implementation of the system under dry cutting conditions took place.

**Keywords:** piezoceramic thick film sensor · lead zirconate titanate (PZT) · cutting force

## 1 Introduction

Cutting forces in machining operations have been studied extensively due to their sensitivity to changes in process states [1]. They have been further used mainly in research activities as input for process optimization, and for monitoring tool wear [2]. The static and dynamic components of force signals are used in the latter case, because the low frequency amplitudes and certain components at higher frequencies increase with higher friction between tool and workpiece when wear is present [3]. Monitoring turning processes is of key relevance for optimizing tool life and reducing workpiece waste by predicting tool breakage, thus optimizing resource use and output quality of the workpiece. This contributes positively to increasing sustainability in turning processes.

© The Author(s) 2023

H. Kohl et al. (Eds.): GCSM 2022, LNME, pp. 30–39, 2023.

[https://doi.org/10.1007/978-3-031-28839-5\\_4](https://doi.org/10.1007/978-3-031-28839-5_4)

For measuring forces and torques in manufacturing technology, piezoelectric sensors, strain gauges, and, occasionally, inductive and capacitive position transducers are utilized [4]. Piezoelectric based plate dynamometers are usually preferred due to their high stiffness and good static properties, such as good linearity and negligible crosstalk [2]. Commercial plate dynamometers, for example the models 9121 or 9119A from Kistler, have been used in several research works in the field of machining process monitoring [5]. A drawback of such systems resides in their relatively limited usable frequency bandwidth before attaining resonance at 0.7 - 1 kHz, caused by their relatively high mass compared to the standard tool-holders (mass ratio of 3:1) [6]. A further limitation for practical applications relates to the high cost of the system.

Some approaches in the literature dealt with the issues of improving integrability, reducing system mass, and improving the usable bandwidth. Klocke et al. [6] proposed a modular sensor concept for integration in a rotating tool-holder for face-milling. The individual sensor modules were tested in a lathe turret and compared with a reference plate dynamometer by performing static and dynamic measurements with the help of an impact hammer. The dynamic limit of the proposed sensor system of 2.1 kHz was obtained by means of a dynamic test under ideal conditions and a value of 1.7 kHz was established under real cutting conditions. This showed an improvement in contrast to the transfer function of a plate dynamometer, which achieved a first resonance peak at approximately 1 kHz. Similar results are presented by Totis et al. in [2, 5].

Drossel et al. [7] proposed a novel concept for measuring cutting forces in milling applications and in the direct vicinity of the indexable insert. The sensor concept consisted of a carbide plate coated with a piezoceramic thick film sensor layer of lead zirconate titanate (PZT), which was mounted behind the tool insert [7]. The high quality of the measured signals was compared to that of signals obtained with a conventional dynamometer, showing the high potential of the approach for improving the integrability of this type of sensors in machine tools, by reducing the required mounting space and the influence on the tool-holder rigidity and mass properties.

This work further investigates the integration of piezoceramic thick film sensors for measuring cutting forces in turning processes. The previous implementation proposed by Drossel et al. was done for milling operations, which focused on the dynamic characteristic of the force signals. The novelty of this work consists in qualifying the sensor-technology for also measuring the quasistatic component of the cutting force signals. The following objectives were pursued: (1) to estimate the performance of the sensor at the integration location in the tool-holder by means of a static structural-piezoelectric coupled simulation, (2) to fabricate and assemble the designed sensor geometry in the tool-holder system and to characterize its static and dynamic properties, (3) to perform cutting tests in turning operations and compare the acquired force signals to those of a reference dynamometer, and (4), to conclude on the performance of the sensing approach and relevant aspects for optimizing the design. The results of this work cover a first step towards qualifying the sensor for quasistatic force measurements. Future work includes extending the sensing principle to a continuous monitoring scenario with the aim of optimizing turning processes in the context of sustainable manufacturing.

## 2 Sensor Design and Simulation

Piezoelectric materials have the property of converting mechanical energy to electrical energy. This occurs by generating an electric polarization (charge) proportionally to the application of a mechanical stress, and it is a natural property of some single crystals like quartz, ferroelectric ceramics (e.g. PZT), and piezoelectric polymers [8]. Models used for simulating the direct piezoelectric effect are defined by coupling the structural and electrical fields occurring in the material. For static analysis relating the output voltage to a given constant strain, piezoelectric materials are modelled considering their structural elasticity, piezoelectric coupling, and dielectric permittivity as follows [8]:

$$\begin{aligned} \{T\} &= [c]\{S\} - [e]\{E\} \\ \{D\} &= [e]^T\{S\} + [\epsilon]\{E\} \end{aligned} \quad (1)$$

In (1),  $\{T\}$ ,  $\{S\}$ ,  $\{D\}$ ,  $\{E\}$ , are the stress, elastic strain, electric flux density, and electric field intensity vectors. The matrixes  $[c]$ ,  $[e]$ ,  $[\epsilon]$  represent the elastic stiffness, the piezoelectric coupling, and the dielectric permittivity respectively.

The previous formulation was implemented in ANSYS-Workbench in order to simulate the charge output of a rectangular PZT thick film sensor geometry with an area of  $10 \times 10 \text{ mm}^2$  and a layer thickness of  $40 \mu\text{m}$ . The sensor geometry and its location between the tool-holder and the tool-holder receptacle is shown in Fig. 1.

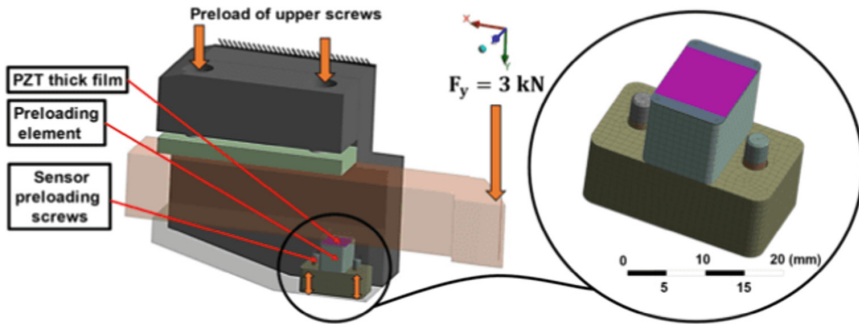


**Fig. 1.** Geometry of PZT thick film sensor integration concept and conditions of static model.

The preferred location of the sensor was qualitatively determined under the criteria of smallest possible distance to the cutting insert in the force transmission path while concurrently maximizing protection against external particles and coolant. The location was also estimated as less susceptible to temperature effects compared to directly below the cutting insert, where the temperature increase is more significant. Further, the attachment of the sensor was simulated by fastening a preloading element.

The static simulation was performed in three steps, corresponding to the application of a 20 kN preload on the upper screws to secure the tool-holder, followed by the application of a 0.5 kN preload on each screw at the preloading element, and a last step corresponding to a vertical force at the tool tip of 3 kN. To complete the definition of the boundary conditions, the receptacle of the tool-holder was fixed in all degrees of freedom, and all contacts between components defined as frictional.

The coupled structural-piezoelectric behavior of the sensor was modelled using elements of the type PLANE226 in ANSYS. For the simulation, the material properties of the PZT thick film material IKTS-PZ 5100 used for the sensor have been applied [9]. The PZT thick film is defined as orthotropic, and the elastic stiffness matrix [c] and coupling piezoelectric matrix [e] are defined as follows:

$$[c] = \begin{bmatrix} c_{11} & c_{12} & c_{13} & c_{14} & c_{15} & c_{16} \\ c_{12} & c_{22} & c_{23} & c_{24} & c_{25} & c_{26} \\ c_{13} & c_{23} & c_{33} & c_{34} & c_{35} & c_{36} \\ c_{14} & c_{24} & c_{34} & c_{44} & c_{45} & c_{46} \\ c_{15} & c_{25} & c_{35} & c_{45} & c_{55} & c_{56} \\ c_{16} & c_{26} & c_{36} & c_{46} & c_{56} & c_{66} \end{bmatrix} = \begin{bmatrix} 12.71 & 7.86 & 7.87 & 0 & 0 & 0 \\ 7.86 & 12.71 & 7.87 & 0 & 0 & 0 \\ 7.87 & 7.87 & 11.11 & 0 & 0 & 0 \\ 0 & 0 & 0 & 2.92 & 0 & 0 \\ 0 & 0 & 0 & 0 & 2.92 & 0 \\ 0 & 0 & 0 & 0 & 0 & 2.42 \end{bmatrix} \cdot 10^{10} \text{ Nm}^{-2}$$

$$[e] = \begin{bmatrix} e_{11} & e_{12} & e_{13} \\ e_{21} & e_{22} & e_{23} \\ e_{31} & e_{32} & e_{33} \\ e_{41} & e_{42} & e_{43} \\ e_{51} & e_{52} & e_{53} \\ e_{61} & e_{62} & e_{63} \end{bmatrix} = \begin{bmatrix} 0 & 0 & -1.7 \\ 0 & 0 & -1.7 \\ 0 & 0 & -16.0 \\ 0 & 11.3 & 0 \\ 11.3 & 0 & 0 \\ 0 & 0 & 0 \end{bmatrix} \cdot \text{Cm}^{-2}$$

To complete the formulation, the dielectric permittivity constants (in F/m)  $\epsilon_0 = 8.85 \cdot 10^{-12}$ ,  $\epsilon_{s1}$  and  $\epsilon_{s2} = 1320 \cdot 10^{-12}$ , and  $\epsilon_{s3} = 1475 \cdot 10^{-12}$  are included. All other components, including the substrate of the sensor, were modelled as steel with an elastic modulus of 200 GPa and a Poisson's ratio of 0.3. The charge output in pC of the model is presented in Fig. 2. The linear behavior suggests a favorable location of the sensor for measuring the cutting force in the 0–3 kN range. An additional criterion for the design consists in not exceeding the depolarization stress of the material of 50 MPa, and which was verified with a simulated maximum value of 26 MPa. Given these results, the sensor design was determined to be suitable for fabrication and testing. The estimated charge output is further used as guideline for selecting the range of the charge amplifier for the characterization of Sect. 3.

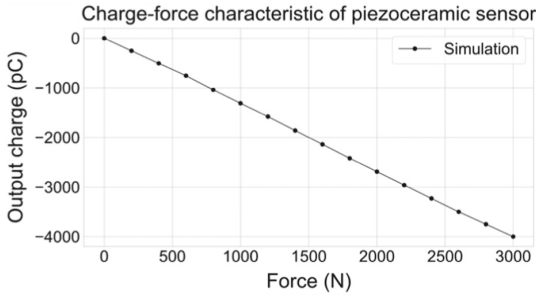


**Fig. 2.** Simulated charge output of piezo ceramic thick film sensor.

### 3 Characterization

Following the simulation, the PZT thick film sensor was fabricated by means of a screen-printing process applied on a substrate of a specially heat-treated steel alloy of the reference 1.4016. The sensor and the adapted geometry of the tool-holder are displayed in Fig. 3(left). The layer set-up comprised a successively printed sequence of dielectric insulation, bottom Au electrode, PZT thick film based on IKTS-PZ 5100 material, top Au electrode, and passivation layer. The layers were sintered at 850°C for 10 min with a total firing cycle time of 60 min. The PZT thick film was built up by repeated screen-printing in the green state to reach a sintered thickness of 40  $\mu\text{m}$ . A polymer-based passivation layer has been printed on top to protect sensor from environmental influences such as cooling lubricants and chips. It has been cured after printing at 150°C for 60 min. The following thicknesses were achieved in the sintered/cured state: (1) dielectric insulation:  $t \sim 25 \mu\text{m}$ , (2) Au bottom electrode:  $t \sim 10 \mu\text{m}$ , (3) PZT thick film:  $t \sim 40 \mu\text{m}$ , (4) Au top electrode:  $t \sim 10 \mu\text{m}$ , (5) Passivation layer:  $t \sim 15 \mu\text{m}$ .

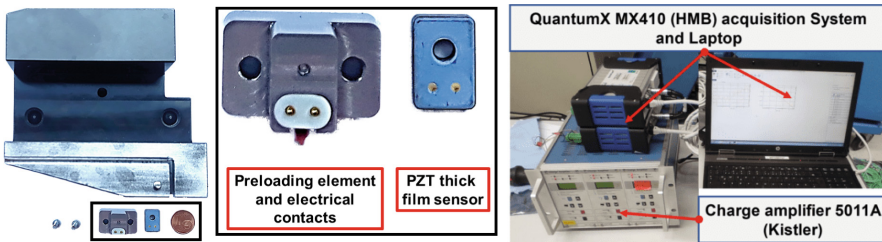


**Fig. 3.** Integration of sensor in tool holder (left) and set up for data collection (right).

#### 3.1 Static Calibration

The assembled prototype was calibrated using a “Zwick-und Roell” universal testing machine with an integrated load cell of the type “Xforce P” (precision class 1 according to ISO 7500). The load cell provided a measuring range of up to 20 kN, a resolution of

$< 0.5\%$ , and a repeatability  $< 1\%$ . For the calibration, a compression load of up to 3 kN was applied at the tip of the tool-holder by means of an axial transmission rod directly connected to the load cell of the machine. For acquiring the output voltage signal of the sensor, a charge amplifier type 5011A from Kistler and a QuantumX MX410 acquisition system from HBM was used (Fig. 3, right). The test was performed using three different rates of application of the force. For each of these, five loading and unloading cycles were performed. The results are presented in Fig. 4.

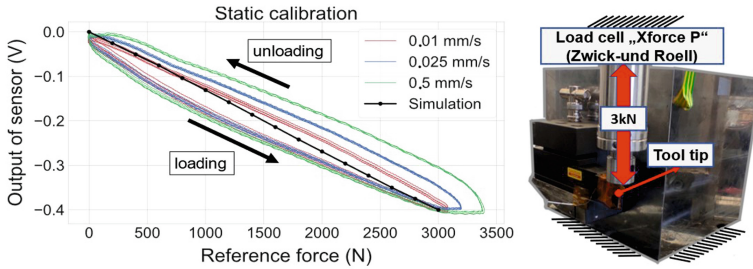


**Fig. 4.** Force at the tool tip and voltage output of sensor (left) and static calibration (right).

The calibration revealed a significant frequency dependent hysteresis of the signal output, which is consistent with the known behavior of ferroelectric ceramics [8]. For a first implementation, only the loading portion was used for calibrating the sensor, assuming a constant slope. As a last remark it should be noted that the simplified static simulation model of Sect. 2 fits reasonably well within the measuring range of the output signals, with the conversion from pC to V being performed by using the conversion factor of the charge amplifier.

### 3.2 Dynamic Characterization

The vibrational response of the measuring system was further investigated by exciting it with an impact hammer to estimate its frequency response function *FRF* [10]. An idealized test set-up was built by attaching the tool system to a steel block, with a mass ratio of 10:1. The first eigenfrequency of the steel-block using this 10-factor criterion was estimated at 8 kHz, which was above the expected eigenfrequency of the tool-holder in the range of 2–3 kHz. To verify this, measurements were performed by using an impact hammer PCB 086C03 combined with an accelerometer Dytran 3273M2. By positioning the accelerometer at one corner of the steel block and below the cutting-insert, two groups of measurements were recorded by exciting both the steel block and the tool holder separately, as shown in Fig. 5(left). Using the outputs of the accelerometer and the impulse hammer, the FRF-parameter accelerance  $A(\omega)$  is defined as the quotient of the acceleration and force responses (Fig. 5, center) [10]. In the majority of the frequency range up to 7.5 kHz the blocks accelerance is ten times lower than that of the measuring system. Also, the isolated block lies above 7.5 kHz, while the first eigenfrequency of the measuring system is around 2.4 kHz. This value of 2.4 kHz is also obtained after

calculating the force transfer function between the output signal of the measuring system and that of the impulse hammer (Fig. 5, right). The result is consistent with the results presented in [2, 6], thus reflecting a potential improvement of the effective bandwidth by roughly a factor two compared to plate-dynamometers.

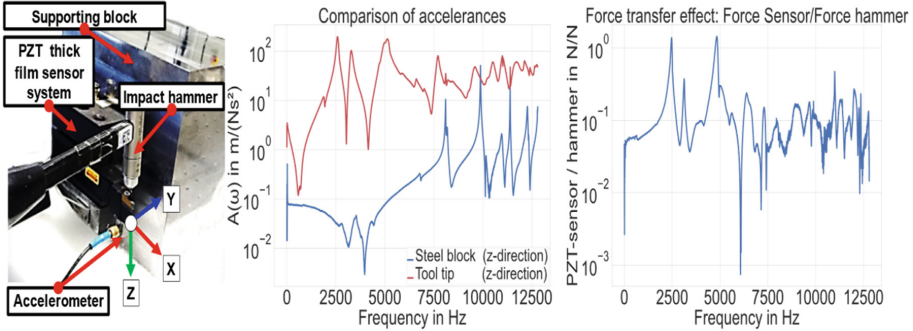


**Fig. 5.** Impact hammer test set-up (left), comparison of acceleration of supporting block and tool-holder (center), and force transfer function of measuring system (right).

### 4 Cutting Tests

Outer diameter step turning operations were performed both with the developed sensor system and with a reference plate dynamometer 9129AA from Kistler. A 40CrMnMoS8-6 steel bar was machined (dry conditions) using a cutting depth of 1 mm, a feed of 0.3 mm/rev, and a cutting speed of 150 m/min. The force signals were acquired using the same settings of the charge amplifier of the static calibration and a sampling rate of 4.8 kHz. Details of the setup are shown in Fig. 6.

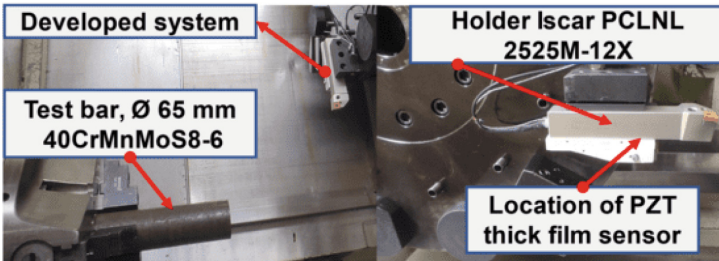


**Fig. 6.** Set-up of developed system in turning test under dry conditions.

The result of the cutting test in the time domain is presented in Fig. 7(left). The cutting force signal of the reference dynamometer (blue line) remains constant as expected for constant cutting parameters. The red curve of the developed system shows in contrast a constant positive drift, which is due to the thermal sensitivity of the sensor at the

measuring location. Two aspects contribute to this: (1) the slight change of the piezoelectric properties of the PZT sensor in dependence of the temperature, and (2) a thermally induced mechanical load on the sensor caused by the linear expansion of the components with increasing temperature. This last assertion is supported by the documentation of the reference dynamometer, which makes mention of previous models facing this thermal effect at a similar sensor location and preload method. Future tests must include a temperature measurement at the location of the sensor and performing tests with coolant. It should be thus determined if a temperature compensation is necessary even after using coolant. Despite the differences of the signals of the new and reference systems, the feasibility of using PZT thick film sensors for measuring quasistatic cutting forces and the potential for improvement was first demonstrated.

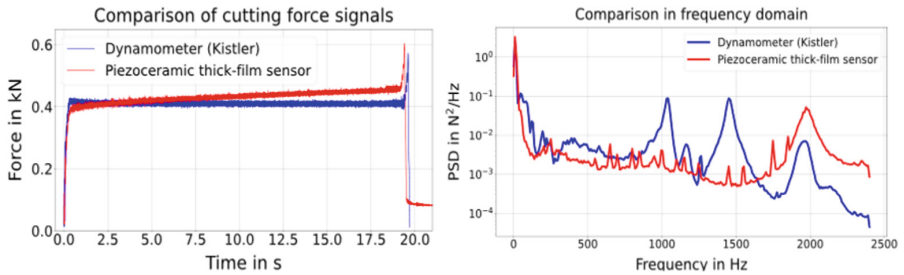


**Fig. 7.** Cutting force signals in time domain (left) and comparison of spectral power densities (PSD) of signals (right), obtained from PZT thick film sensor and reference dynamometer (Color figure online).

The performance of both systems in the frequency domain is compared in Fig. 7 (right) by means of a power density spectrum. A first major peak on the signal of the PZT thick film sensor (red line) is observed at around 2 kHz, roughly corresponding to the 2.4 kHz resonance frequency of the ideally supported setup for the impact hammer test of Sect. 3. The first major peak on the case of the reference dynamometer occurs at around 1 kHz. The analysis on the frequency domain might suggest an effective usable bandwidth of the system based on the PZT thick film sensor twice as large as that of the reference dynamometer, with an additional impact hammer test with the dynamometer in order to confirm the result. The plausibility of this assertion is supported by similar literature results as presented in [2, 5, 6]. At last, an estimate of the signal-to-noise-ratio (SNR) was calculated by defining noise as the portion of the signal in idle state (no cutting, spindle off) and the sensor force signal in the frequency band above 10 Hz. The SNR-values calculated using the RMS of the signals obtained with the Kistler dynamometer and with the developed system were 28 and 22 dB respectively.

## 5 Conclusion and Future Work

This work presented a first attempt for integrating PZT thick film sensors for the purpose of measuring cutting forces in turning processes. A new concept of the sensor

was simulated prior to its fabrication, with the output of the simulation lying within the range of the static calibration of the system. Finally, the system was tested under cutting conditions and compared to a reference dynamometer. The main result of this work is the demonstration of the feasibility of the PZT thick film sensor for measuring quasistatic forces in turning processes. The potential benefits of the system compared to the reference dynamometer consist in an overall cost reduction (which is itself one of the biggest challenges for using near-process force measurements in monitoring of turning processes), a mass reduction by a 3:1 ratio, a potential increase of the bandwidth, and a higher flexibility for integrating the sensors in general tool holder geometries by specifically designing the sensor geometry. Additional aspects to be considered for further qualifying the PZT thick film sensors for process monitoring consist in: (1) extension of FE-analysis to include transient thermal effects in order to evaluate optimal sensor location, (2) evaluation of compensation of temperature drift by using coolant and/or compensation using temperature sensor, (3) analysis of the impact of coolant on the signal quality, (4) development of strategies for compensating the frequency dependent hysteresis, and (5) performing continuous measurements of entire tool life and evaluating sensitivity of signals to wear states compared to reference dynamometer.

## References

1. Teti, R., Jemielniak, K., O'Donnell, G., Dornfeld, D.: Advanced monitoring of machining operations. *CIRP Ann.* **59**(2), 717–739 (2010)
2. Totis, G., Sortino, M.: Development of a modular dynamometer for triaxial cutting force measurement in turning. *Int. J. Mach. Tools Manuf.* **51**(1), 34–42 (2011)
3. Scheffer, C., Kratz, H., Heyns, P.S., Klocke, F.: Development of a tool wear-monitoring system for hard turning. *Int. J. Mach. Tools Manuf.* **43**(10), 973–985 (2003)
4. Klocke, F.: *Manufacturing Processes 1: Cutting*. Springer-Verlag, Berlin (2018)
5. Totis, G., Wirtz, G., Sortino, M., Veselovac, D., Kuljanic, E., Klocke, F.: Development of a dynamometer for measuring individual cutting edge forces in face milling. *Mech. Syst. Signal Process.* **24**(6), 1844–1857 (2010)
6. Klocke, F., Kuljanic, E., Veselovac, D., Sortino, M., Wirtz, G., Totis, G.: Development of an intelligent cutter for face milling. *Strain* **14**, 15 (2008)
7. Drossel, W.-G., Gebhardt, S., Bucht, A., Kranz, B., Schneider, J., Ettrichraetz, M.: Performance of a new piezoceramic thick film sensor for measurement and control of cutting forces during milling. *CIRP Ann.* **67**(1), 45–48 (2018)
8. Dahiya, R.S., Valle, M.: *Robotic Tactile Sensing*. Springer, Dordrecht (2013)
9. Ernst, D., Bramlage, B., Gebhardt, S.E., Schönecker, A.J.: High performance PZT thick film actuators using in plane polarisation. *Adv. Appl. Ceram.* **114**(4), 237–242 (2015)
10. Ewins, D.J.: *Theory and Practice of Modal Testing*. Modal Testing Unit, Mechanical Engineering, Imperial College (1983)

**Open Access** This chapter is licensed under the terms of the Creative Commons Attribution 4.0 International License (<http://creativecommons.org/licenses/by/4.0/>), which permits use, sharing, adaptation, distribution and reproduction in any medium or format, as long as you give appropriate credit to the original author(s) and the source, provide a link to the Creative Commons license and indicate if changes were made.

The images or other third party material in this chapter are included in the chapter's Creative Commons license, unless indicated otherwise in a credit line to the material. If material is not included in the chapter's Creative Commons license and your intended use is not permitted by statutory regulation or exceeds the permitted use, you will need to obtain permission directly from the copyright holder.

